Materials Today Chemistry 18 (2020) 100371

Contents lists available at ScienceDirect

Materials Today Chemistry

journal homepage: www.journals.elsevier.com/materials-today-chemistry/

Modification of a phase-inhomogeneous alumina support of a palladium catalyst. Part I: effect of the amorphous phase on the textural and acidic characteristics of alumina and methods for controlling its phase homogeneity

A. Boretskaya [a, *], I. Il'yasov [a], S. Egorova [a], A. Popov [b], A. Lamberov [a]

[a] Alexander Butlerov Institute of Chemistry, Kazan Federal University, Kazan, 420008, Russia
[b] Chemistry Department, Lomonosov Moscow State University, Moscow, 119234, Russia

ARTICLE INFO

Article history:
Received 16 July 2020
Received in revised form
13 September 2020
Accepted 14 September 2020
Available online 13 October 2020

Keywords:
Amorphous alumina
Crystalline alumina
Chemical modification
Hydrothermal treatment

ABSTRACT

The contribution of the amorphous phase in aluminum hydroxide and alumina to their properties was investigated in this work. It was shown that the amorphous phase in aluminum hydroxide is stabilized by alumoxanes, and it is a source of a finely porous component and capable of increasing the surface area by ~78%. In γ-Al_2O_3, amorphous alumina raises the surface area and the acidity. It was established that the method of chemical modification does not change the phase inhomogeneity but allows adjusting the acid properties while maintaining the high specific surface area. It was shown that the amorphous phase is more reactive when processing phase-inhomogeneous aluminum hydroxide with acetic acid. Crystallization of amorphous alumina as a result of high-temperature treatment of phase-inhomogeneous aluminum hydroxide is accompanied by significant decrease in specific surface area and acidity.

1. Introduction

Aluminum oxides are widely used as adsorbents, catalysts, and catalyst supports in pharmaceutical [1] and organic chemistry practices [2], oil refining and petrochemical processes [3,4]. This is because of the presence of various modifications of alumina, characterized by thermal stability, textural, and acid-base properties [5,6]. These characteristics are very important when using aluminum oxides as catalyst supports, because structural and charge properties of the active component are formed as a result of the metal-support interaction effect [7–9]. To fix finely dispersed particles of the active component on the catalyst surface, alumina must have a developed specific surface area and sufficient concentration of acid-base sites, which is typical for a low-temperature modification, such as γ-Al_2O_3 [10,11]. It is known that the precursors of aluminum oxides are aluminum hydroxides, which in mass production are obtained by hydrolysis of inorganic or organic aluminum salts. However, the hydrolysis rate of each successive step decreases. The values of the negative logarithm of the hydrolysis constant of inorganic aluminum salts from steps 1 to 3 are about 6, 11 and 17, respectively [12]. Aluminum hydroxides with a low content of metal impurities are obtained by hydrolysis of aluminum alkoxides. In this case, the hydrolysis rate largely depends on the nature of the aluminum alkoxides and the coordination number of aluminum. Aluminum alkoxides rapidly undergo oligomerization to form more stable forms (di-, tetra- or octamers) [13]. Bridge aluminum alkoxides are more resistant to hydrolysis than terminal ones [14]. The hydrolysis rate decreases as the alkyl chain lengthens and increases in the presence of acid-type catalysts protonating negatively charged alkoxide groups [15]. However, the use of catalysts in reactions with a low mole ratio of water to alkoxide (to obtain boehmite) often leads to formation of gel-like products. Products of incomplete hydrolysis of aluminum alkoxides are referred to as alumoxanes [16]. They have less reactivity and represent oligomers or crystalline substances, most of which are non-stoichiometric in composition and consist of boehmite-like aluminum-oxygen core and various functional groups (alkyls, carboxyls), which allows them to stabilize in the structure of boehmite itself [17]. This prevents complete crystallizing of the boehmite, contributing to the formation of amorphous aluminum hydroxide, which is characterized by small particles with small and often irregular pores between them, such structure is often called a

* Corresponding author.
E-mail address: ger-avg91@mail.ru (A. Boretskaya).

https://doi.org/10.1016/j.mtchem.2020.100371
2468-5194/

wormhole [16]. The decomposition of alumoxanes at the stage of calcination of aluminum hydroxide leads to the formation of amorphous alumina or γ-Al_2O_3 at temperatures above 300 °C [18,19]. Therefore, hydrolysis reaction products are often phase-inhomogeneous, because they contain crystalline and amorphous aluminum hydroxides. Crystalline aluminum hydroxide is dehydrated into the low-temperature form of crystalline alumina at temperatures of 300–500 °C [20,21]. Amorphous aluminum hydroxide in the range from 250 to ~700 °C is dehydrated into amorphous aluminum oxide. That is why, the heat treatment of phase-inhomogeneous aluminum hydroxide for obtaining a low-temperature modification will also be accompanied by formation of a phase-inhomogeneous aluminum oxide which consists of γ-Al_2O_3 and amorphous alumina. To date, studies of the properties of amorphous alumina are given for its 100% content case. It has unique properties and is interesting for having high dielectric constant [22–24], used in fluorescent and optical devices [25,26], and in the getting of crystalline materials [27–29]. Therefore, only the physical and optical properties of fully amorphous alumina have been studied. However, when using aluminas as catalysts or their supports, the contribution of amorphous alumina is neglected, but this may be the cause of conflicting research results. Phase inhomogeneity will reduce the reproducibility of the textural and acid characteristics of alumina, the properties of supported metal particles and, consequently, their catalytic activity. The inability to identify amorphous alumina in the crystalline composition makes it impossible to determine its contribution to both the properties of alumina and the active component of the catalyst. Amorphous alumina can only be identified in some cases by the presence of a five-coordinate aluminum cation in the 28–40 ppm region on the ^{27}Al NMR spectrum [30–34]. On the X-ray diffraction patterns and IR spectra there are no bands characteristic of amorphous alumina, which does not allow it to be detected. Earlier [35], we proposed a method for identifying amorphous alumina in the composition of γ-Al_2O_3, based on various phase labilities. As a result of hydrothermal treatment (HTT) of phase-inhomogeneous alumina, two boehmites with different temperatures of phase transformation into γ-Al_2O_3 were discovered. It is accompanied by two peaks of endothermic effect at 482 and 514 °C on the DSC curve. So, the sequence of these actions: a short-term HTT of alumina and recording of the DSC curve represents a method for detecting phase inhomogeneity of alumina, including identification of amorphous alumina.

Common methods for modifying alumina are its chemical or high-temperature treatment. The interaction of modifying ions mainly proceeds by the mechanism of electrophilic or nucleophilic substitution of surface hydroxyls or protons in their composition [36,37]. However, the literature shows the data on the effect of modifiers on the properties of crystalline aluminum oxides, while the amorphous phase is often accessory. To prevent from additional stages of the synthesis of aluminum oxides, it is advisable to introduce chemical modifiers into aluminum hydroxides. Moreover, the various phases in the composition of the aluminum hydroxide are likely to have different reactivity. In this article, we propose understanding the way chemical modification affects the phase composition and properties of a phase-inhomogeneous aluminum hydroxide and alumina obtained from it. In the case of high-temperature processing, crystallization of amorphous alumina into crystalline alumina occurs at temperatures above 700 °C [32,38]. However, this is accompanied by a decrease in the specific surface area and concentration of acid sites.

Thus, when creating catalytic systems with good reproducibility, it is necessary to consider the following: (1) what is the contribution of the amorphous phase and various methods of modifying aluminum oxides to (i) morphology, textural and acid properties of aluminum oxide, (ii) characteristics of the active component, and (iii) its performance; (2) controlling the phase homogeneity of hydroxides and aluminum oxides. In this article, we will show the way the phase composition, parameters of the porous structure, and the concentration of acid sites of aluminum oxides change as a result of chemical modification and heat treatment of a phase-inhomogeneous aluminum hydroxide. The contribution of the amorphous phase to these properties was also studied. In the second part of our work, we show the way the presence of amorphous alumina and a change in the properties of an alumina support as a result of various methods of its modification affect the catalytic activity of palladium particles in the partial hydrogenation of unsaturated hydrocarbons.

2. Materials and methods

The initial aluminum hydroxide (denoted as AH-1) represented a powder form of commercial sample of alumina hydroxide obtained by hydrolysis of alumina alkoxides. According to the passport data, it contains silicon dioxide (SiO_2) ~120 ppm, iron sesquioxide (Fe_2O) ~100 ppm, calcium oxide (CaO) ~50 ppm, magnesium oxide (MgO) ~50 ppm, sodium oxide (Na_2O) ~20 ppm, and potassium oxide (K_2O) ~20 ppm. Chemical modification of AH-1 was carried out with water solution of acidic or basic modifiers. The acidic modifiers were acetic acid (the sample denoted as AH-Ac) and ammonium fluoride (AH-F), and the basic modifiers were sodium hydroxide (AH-Na) and cesium nitrate (AH-Cs). The ratio of acetic acid to AH-1 was 0.15 mol–1 mol, and the ratio of the modifier ion (fluorine, sodium or cesium) to AH-1 was 0.03 mol–1 mol. This concentration of modifying additives was chosen in order to obtain alumina oxides with close specific surface area but different effects on the acidity of the support, which play an important role in the formation of the active component (palladium). Acetic acid is widely used as a peptizing agent, so this concentration of acetic acid has been used. The solution of modifier was mixed with AH-1 powder at 85 °C and subsequently dried at 120 °C. These samples of aluminum hydroxides, except for AH-Cs, were calcined at 550 °C (the heating rate was 2 °C/min) within 1 h at an atmospheric pressure to obtain alumina oxides. This temperature corresponds to the completion of the phase transformation of boehmite to γ-Al_2O_3, according to the data of differential scanning calorimetry (DSC) analysis. The AH-Cs was calcined at 650 °C to remove the nitro group. The obtained calcined samples were labeled, starting with a prefix of AO followed by the modifier ion. The unmodified aluminum oxide was denoted as AO-1. The hydrothermal treatment (HTT) was carried out on AH-1 and AO-1 samples within 4 and 1 h, respectively. The obtained samples were labeled as AH-HTT and AO-HTT, respectively. The hydrothermal treatment was carried out with seven times excess of water in stainless steel autoclave (V = 200 mL, without stirring) at 150 °C (2 °C/min). The pressure reached 4 atm. After HTT the samples were dried at 120 °C within 2 h and were calcined at 550 °C within 1 h at an atmospheric pressure to obtain the AO-2 (from AH-HTT) and AO-3 (from AO-HTT) samples. The high-temperature treatment of AH-1 was carried out at 800 (2 h), 900 (4 h) and 1100 °C (4 h) to obtain aluminum oxides labeled as AO-800, AO-900 and AO-1100, respectively.

X-ray diffraction (XRD) studies of the samples were performed using the MiniFlex 600 diffractometer (Rigaku, Japan) equipped with a D/teX Ultra detector. In this experiment, Cu Kα radiation (40 kV, 15 mA) was used and the data were collected at room temperature in the range of 2θ angle from 2 to 100° with a step of 0.02° and exposure time at each point of 0.24 s without sample rotation. Crystal sizes (coherent scattering regions, CSRs) were evaluated using the Scherrer formula for the (020) plane of

aluminum hydroxides, for the (440) plane of γ-Al_2O_3 samples and for the (104) plane of AO-1100. The molar ratio of H_2O to Al_2O_3 (the quantity of interlayer water), ν, was calculated by the (020) plane.

Simultaneous thermogravimetry and differential scanning calorimetry (TG/DSC) analysis of the samples and mass spectrometric (MS) evolved gas analysis were performed using the thermoanalyzer STA 449F1 Jupiter (Netzsch, Germany) coupled with quadrupolar mass-spectrometer QMS 403 D Aeolos (Netzsch, Germany) at the temperature range from 30 to 1000 °C (10 °C/min) in Pt/Rh crucible and an argon atmospheric with a total flow rate of 75 mL/min. The results were processed with the NETZSCH Proteus software. The molecular weight of alumina hydroxides was calculated taking into account the amount of interlayer water (Mr = Mr(Al_2O_3) + ν*Mr(H_2O), g/mol). The concentrations of boehmite (ω(B)) were found from the weight loss of the second endotherm on the derivative thermogravimetric (DTG) curve (dehydration of boehmite) (Δw_3, %) with deducted weight loss after removal of the physically adsorption water (Δw_1, %) and dehydroxylation of the alumina at 550 °C (Δw_4, %) [35].

Measurement of weight changes with the simultaneous identification of the resulting volatile components during the heat treatment of aluminum hydroxides under air from room temperature to 700 °C (10 °C/min) was performed using the combination of thermal analysis with Fourier transform infrared (FTIR) spectroscopy on a synchronous thermal analyzer STA 409 PC Luxx (Netzsch), combined with the external gas cell of the Tensor 27 FTIR spectrometer.

Carbon content was quantified on the HORIBA EMIA-510 with a thermal conductivity detector by burning samples (~0.3 g) in oxygen atmospheric at 1450 °C for 60 s. Before this analysis, the samples were dried at 120 °C.

The infrared (IR) spectra of aluminum hydroxides were recorded on a Spectrum 400 Fourier spectrometer (Perkin Elmer) with an ATR attachment, KRS-5, with a spectral resolution of 1 cm^{-1}, accumulation of 16 scans, shooting range of 4000–400 cm^{-1}.

The specific surface area (S) (calculated with the Brunauer–Emmett–Teller method) [39] and the pore volume (V) (calculated with the Barrett–Joyner–Halenda method) were determined using a multipurpose ASAP 2400 analyzer (Micromeritics, USA). Adsorption isotherms were obtained at −196 °C (77 K) after the degassing of aluminum hydroxides at 150 °C and of aluminum oxides at 250 °C under the residual pressure of 0.013 Pa. The surface area distribution over the pore diameters (dS/dD) and pore size distribution (dV/dD) were determined by the curve of desorption isotherm using the Barrett–Joyner–Halenda method [40].

The total acidity of the synthesized aluminum oxides was determined using the AutoChem 2950 HP analyzer. About 0.5 g of the samples were loaded into a quartz reactor with the following degassing of the instrument in an electric furnace at 550 °C (10 °C/min). The flow rate of carrier gas (He) was 10 ml/min. The support was saturated with a mixture of 10% ammonia (NH_3) in helium (He) at room temperature for 1 h. The physically adsorbed ammonia was removed by helium flow at 100 °C for 30 min. After analysis, the sample was cooled to room temperature in a helium flow. Temperature programmed desorption of ammonia (NH_3 TPD) was carried out in the range from room temperature to 700 °C (10 °C/min). Calculations of NH_3 TPD data on the distribution of acid sites were performed according to the method given in the research [41].

Infrared spectroscopy of adsorbed pyridine was performed using the Nicolet protégé 460 with an optical resolution of 4 cm^{-1} in the region from 4000 to 400 cm^{-1}. The samples in the form of disks (diameter is 1.6 cm, ρ ~ 10 mg/cm^2) were activated in an IR cell at 400 °C (7.5 °C/min) within 2 h and pressure of 10^{-5} torr. Adsorption of probe molecules was carried out at 150 °C and pressure of 2 torr of pyridine within 30 min. At the end of the adsorption cycle, pyridine desorption was performed at 150 °C within 15 min. The concentration of Bronsted and Lewis acid sites was determined by the intensity of adsorbed pyridine bands (1545 and 1450 cm^{-1}, respectively), extinction coefficients were used according to the work [42].

3. Results

3.1. Investigation of main properties of the initial aluminum hydroxide

The X-ray diffraction pattern of the initial alumina hydroxide contains lines, which are characteristic of boehmite (γ-AlOOH) (International Centre for Diffraction Data (ICDD) PDF card 00-049-0133) (Fig. 1). Interlayer water is 1.19 mol on 1 mol of alumina oxide. However, a high value of (020) interplanar spacing, 0.638 nm, low intensity and broadening lines indicate a low degree of sample crystallinity, possibly due to the presence of an amorphous phase [43]. Thus, in transmission electron microscopy (TEM) images, which were presented in our earlier work [35], in addition to well-crystallized small plate-like particles, there are loose non-crystallized, amorphous sections, causing wide ring on micro-diffraction patterns.

The calcination of AH-1 followed by the processes of dehydration and dehydroxylation. Two pronounced endothermic effects are observed on the DSC curve under argon at temperature between 100 and 207 °C (I range) and between 370 and 536 °C (III range) (Fig. 2 a).

The first endothermic effect with peak at 131 °C is due to the removal of sorbed water and carbon dioxide from the pores of aluminum hydroxide, as evidenced by the responses of the mass spectrometer with charge numbers m/z = 18 and 44, respectively. An asymmetric broadening (shoulder) was found on the DSC curve in the range from 208 to 369 °C (II range), followed by the endothermic effect of the phase transformation of boehmite into γ-Al_2O_3 with a peak at 466 °C (III region). This shoulder may be due to dehydration of pseudoboehmite in γ-Al_2O_3 or dehydration of amorphous aluminum hydroxide ($Al(OH)_3^{Am}$) to amorphous oxide ($Al_2O_3^{Am}$). However, in our case, according to the results of XRD pattern, calcination of the AH-1 at 370 °C does not lead to formation of γ-Al_2O_3. The shoulder on the DSC curve of the sample calcined at 370 °C was not observed, but the temperature of phase transformation of boehmite and weight loss on the TG curve during this process have almost no changes.

The crystallization temperature of amorphous alumina oxide on the DSC curves at temperatures above 550 °C (IV range) is not detected due to low value of the reaction enthalpy or the broadened effect of low intensity. The weight loss in this range is due to the dehydroxylation of alumina surface. During the simultaneous DSC analysis and IR spectroscopy under air for AH-1 sample carbon dioxide liberation was registered (Fig. 3). It was formed as a result of alumoxanes oxidation. The content of 0.23 % wt. carbon in the AH-1 and characteristic bands at 1629 and 1379 cm^{-1} (Fig. 4) in the IR spectrum confirm the presence of alumoxanes [44].

The nitrogen adsorption-desorption isotherm of AH-1 (Fig. 5a) corresponds to the IV type in the classification of S. Brunauer, L. Deming, U. Deming and E. Teller and indicates the presence of mesopores. Within the IUPAC classification, the hysteresis loop of this isotherm corresponds to the H_2 type characteristic of slit-shaped and cylindrical pores. According to the analysis of the t-plot (Fig. 5b), there are no micropores and the upward deviation of the graph in the region t ≥ 0.5 nm is due to the occurrence of capillary condensation in the mesopores [40].

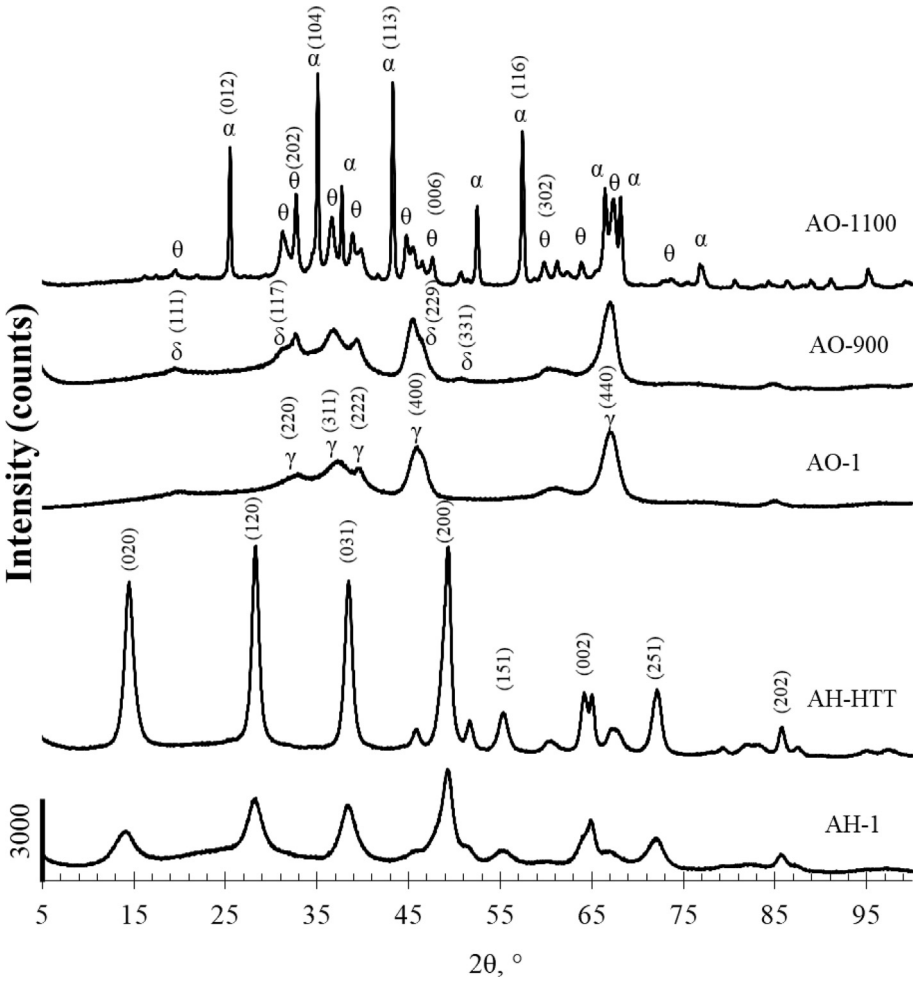

Fig. 1. X-ray diffraction patterns.

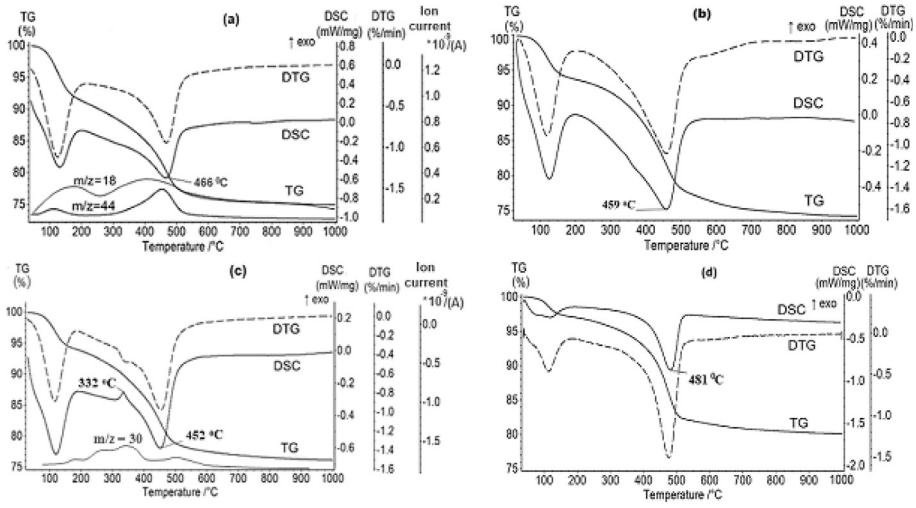

Fig. 2. TG/DSC curves (under argon) of the alumina hydroxides: AH-1 (a), AH-Ac (b), AH-Cs (c) and AH-HTT (d).

Initial aluminum hydroxide is characterized by a high specific surface area, 261 m^2/g, a pore volume of 0.37 cm^3/g, and two maxima on the dS/dD curve at 3.8 and 4.6 nm (Fig. 5c) and the similar maxima on the dV/dD curve.

Thus, based on the obtained results the AH-1 sample is phase-inhomogeneous and consists of 62% boehmite and 38% amorphous phase. The latter is stabilized by the products of incomplete hydrolysis of aluminum alkoxides (alumoxanes).

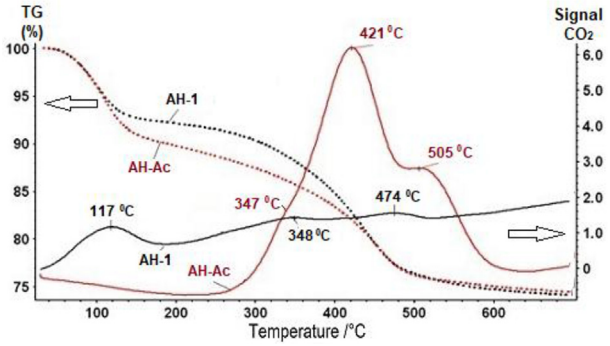

Fig. 3. TG and CO_2 evolution curves of AH-1 and AH-Ac samples (under air).

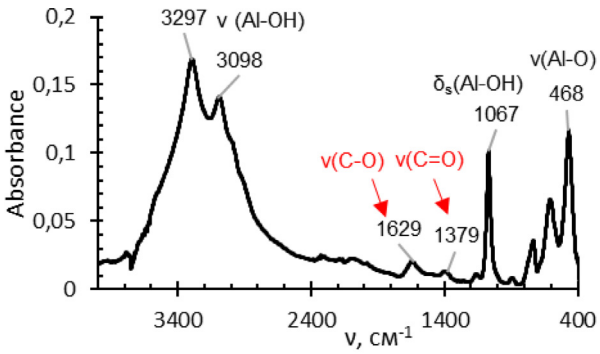

Fig. 4. IR spectrum of AH-1 sample.

modifiers do not affect the phase composition and the amorphous phase is still present. For modified samples a decrease in the content of interlayer water and a slight increase in the crystallite size are observed (Table 1).

Based on the nitrogen adsorption-desorption results, the modification does not lead to a change in the shape of the pores, because the type of isotherms tallies with that for unmodified sample (Fig. 5a).

The sample treated with acetic acid is characterized by a weak specific interaction of the adsorbate with the surface of the modified hydroxide, as evidenced by the intersection of the straight−line portion of the t-plot with the ordinate in the region of negative values (Fig. 5d). This is probably due to the interaction of aluminum hydroxide with a modifier and the formation of aluminum acetate salts. During the treatment of the aluminum hydroxide by acetic acid, the coagulation contacts between the particles are destroyed and the structural elements with diameter pores of ~5 nm are disaggregated. It is accompanied by disappearance of the maximum with this value on the dS/dD and dV/dD curves and the formation of a monomodal porous structure with maximum at 3.8 nm (Table 1, Fig. 5c for AH-Ac). More dense packing of particles and an increase in the proportion of pores with a diameter of less than 4 nm lead to a decrease in the porometry capacity of pore volume by 22%. For the sample modified with sodium hydroxide a surface area decreases by 18% (Table 1), and the maximum intensity on dS/dD curve decreases (Fig. 5c for AH-Na). This is due to the partial replacement of protons surface hydroxyl groups of boehmite with sodium ions, which slows down the crystal growth along the (020) plane (Table 1). For the rest of the samples, the changes in the parameters of the porous structure are

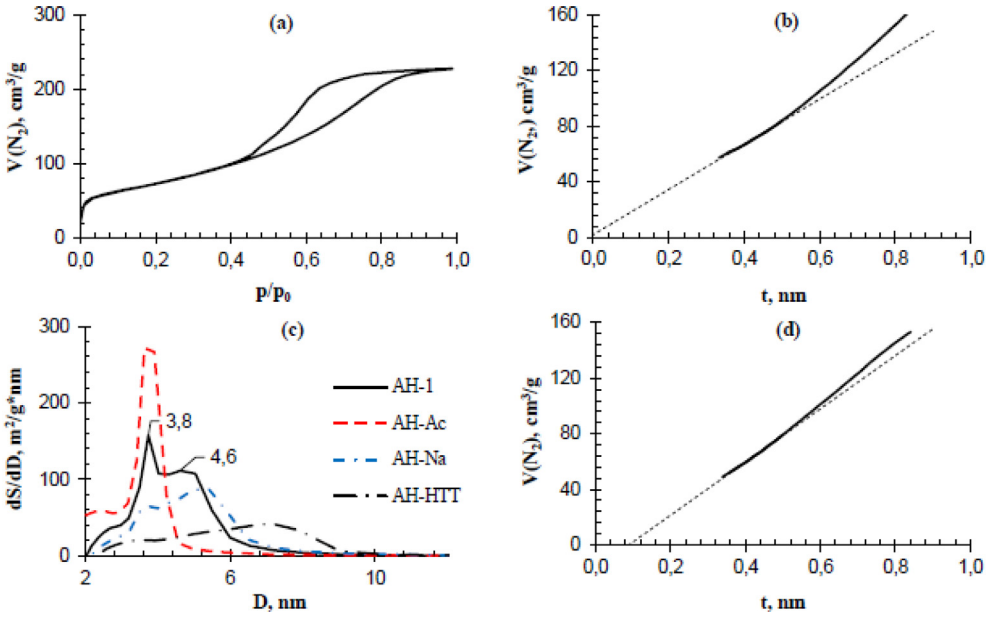

Fig. 5. N_2 adsorption-desorption isotherm (a) and t-plot (b) of AH-1 sample, the curves of surface area distribution over pore diameter of the aluminum hydroxides (c) and t-plot of AH-Ac (d).

3.2. Influence of chemical modification on the phase composition and textural characteristics of phase-inhomogeneous aluminum hydroxide

According to the XRD data, the diffraction patterns of modified aluminum hydroxides have the same set of lines as the initial sample and correspond to boehmite. The line intensities and measures of 2θ angles do not change, which indicates that the less significant and the bimodal distribution of the specific surface area (Table 1) and pore volume is preserved, similar to the initial aluminum hydroxide.

The effect of acidic and basic additives on the phase transformations of aluminum hydroxide was studied by the TG/DSC method under argon and air. On the DSC curves of modified aluminum hydroxides, two endothermic effects and a shoulder are identified, as for the AH-1 sample (Fig. 2a). Calculations based on

Table 1
The phase composition, crystal size and textural characteristics.

Sample	Phase composition	CSR[a], nm	S[b], m^2/g	V[c], cm^3/g	Distribution of S over pore diameter, %			D_{max}[d], nm
					2–4 nm	4–10 nm	> 10 nm	
AH-1	$Al(OH)_3^{Am}$ + γ-AlOOH	3.9	261	0.37	55	202	4	3.8; 4.6
AH-Ac		4.7	253	0,29	95	156	2	3,9
AH-F		4.7	257	0.37	53	199	5	3.8; 5.0
AH-Na		4.1	215	0.34	32	175	8	3.8; 5.4
AH-Cs		4.7	258	0.32	41	209	8	3.8; 5.1
AH-HTT	γ-AlOOH	8.9	147	0.29	13	123	11	7.1
AO-1	$Al_2O_3^{Am}$ + γ-Al_2O_3	4.4	191	0.49	–	130	61	7.9
AO-Ac		5.2	232	0.45	12	214	6	5.8
AO-F		5.0	210	0.45	2	195	13	6.4
AO-Na		4.9	226	0.42	6	193	27	6.5
AO-Cs		5.2	200	0.40	5	172	23	6.4
AO-2	γ-Al_2O_3	5.6	169	0.41	4	93	72	8.9
AO-3		5.0	217	0.45	7	196	14	6.4
AO-800		5.6	149	0.50	–	31	118	10.2
AO-900	(γ+δ)-Al_2O_3	7.5	133	0.47	–	18	115	10.1
AO-1100	(θ+α)-Al_2O_3	46.3	63	0.23	–	9	54	10.7

[a] Coherent scattering regions, corresponds to the crystal size according to the XRD data.
[b] Specific surface area.
[c] Pore volume.
[d] Maximum on the dS/dD curve.

the weight loss on the TG curves at the inflection points (region III in Table 2) showed that the content of boehmite phase in the modified samples is similar to the initial aluminum hydroxide, except for the sample treated with acetic acid.

For the AH-Ac sample an increase in the temperature interval on the DSC curve in the III region with broadening of the endothermic effect of the phase transformation of boehmite with a peak at 459 °C and a larger value of the weight loss on the TG curve (Fig. 2b, Table 2) are observed. This is due to the predominant interaction of the modifier with the most labile phase — the amorphous component — followed by formation of aluminum acetate salts, which decompose in the temperature range from 250 to 550 °C to amorphous alumina [46,47]. The decomposition of salts is accompanied by formation of carbon dioxide with maxima at 347, 421 and 505 °C (peak at 117 °C is characteristic of the sorbed gas) on the curve of its evolution (Fig. 3).

For other modified aluminum hydroxides, the curves of carbon dioxide evolution in the air are similar to the AH-1 sample (Fig. 3 a). On the DSC curve of the AH-Cs sample an exothermic effect with a maximum at 332 °C is observed, due to the decomposition of the nitrate ion, as evidenced by the response of the mass spectrometer $m/z = 30$ (Fig. 2c), which ends at 650 °C.

On the DSC curves of AH-1 and modified samples the phase transformation of boehmite into γ-Al_2O_3 is completed up to 550 °C.

Table 2
The value of interlayer water (ν) and results of TG/DSC analysis (under air).

Sample	ν	II range	III range				IV range
		Δw_2[a], %	T.R.[b], °C	T_{peak}[c], °C	Δw_3, %	ω(B)[d], %	Δw_4, %
AH-1	1.19	4.7	370–536	466	9.6	62	1.9
AH-Ac	1.13	3.0	334–532	459	13.4[e]	89	3.1
AH-F	1.13	5.2	403–550	475	9.7	65	2.9
AH-Na	1.17	5.5	367–532	455	9.5	61	2.1
AH-Cs	1.13	6.3	336–541	452	9.6	63	2.0
AH-HTT	1.04	3.0	370–520	481	13.1	100	2.3

[a] The weight loss in the appropriate range.
[b] Temperature range of the curves.
[c] The peak temperature of the endothermic effect.
[d] The content of boehmite.
[e] The area of simultaneous processes of boehmite dehydration and decomposition of aluminum acetates.

The complete decomposition of alumoxanes and modifier counterions is completed at 650 °C for AH-Cs and at 550 °C for other aluminum hydroxide samples. Therefore, these temperatures were used to obtain corresponding aluminum oxides.

3.3. Investigation of phase composition and textural characteristics of the chemical modified aluminum oxides

The heat treatment of unmodified and modified aluminum hydroxides at 550–650 °C is accompanied by formation of phase-inhomogeneous aluminum oxides. It consists of γ-Al_2O_3 and amorphous aluminum oxide, which are formed as a result of the following reaction:

$$2Al(OH)_3^{Am} + 2\gamma\text{-AlOOH} \rightarrow Al_2O_3^{Am} + \gamma\text{-}Al_2O_3 + 4H_2O.$$

The presence of γ-Al_2O_3 is confirmed by the characteristic reflections on the XRD patterns (ICDD PDF card 00-029-0063) of the obtained samples. For modified aluminas a slight increase in the size of CSR (Table 3) is observed.

Dehydration of amorphous aluminum hydroxide at 550 °C, leads to the formation of amorphous aluminum oxide. Therefore, the content of the amorphous phase in aluminum hydroxide corresponds to the same content in aluminum oxide.

Phase transformations of aluminum hydroxides are accompanied by splicing of microslits (~3.8 nm in diameter) and slugging of fine particles with the formation of new Al–O–Al bonds and formation of a denser structure of alumina. It leads to transformation of the bimodal porous system into a monomodal one with a maximum on the dS/dD (Fig. 6a and b, Table 1) and dV/dD curves in the pore region of a larger diameter and an increase in the pore volume. AO-Ac sample has the highest value of the specific surface area due to the dehydration of the precursor with a smaller size of the structure-forming fragments. For samples AO-F, AO-Na and AO-Cs an increase in the contribution of pores with a diameter of 4–10 nm in specific surface area may be induced by formation of a denser packing of particles due to an occurrence of the ionic nature of the chemical bond in them. In general, there are no significant changes in the textural characteristics (Table 1).

Table 3
The temperature of complete ammonia desorption (T_d^{NH3}), total acid sites concentration ($\sum N$) and their distribution on the energy of ammonia desorption (E_d), according to the NH_3 TPD results.

Sample	T_d^{NH3}, °C	Acid sites concentration, μmol/g			
		$\sum N$	Weak E_d < 100 kJ/mol	Medium 100 ≤ E_d < 150 kJ/mol	Strong E_d ≥ 150 kJ/mol
AO-1	819	819	163	539	117
AO-Ac	688	1044	177	643	224
AO-F	536	853	159	541	153
AO-Na	455	552	99	394	59
AO-Cs	463	356	64	260	32
AO-2	505	579	105	403	71
AO-3	653	876	142	570	164
AO-800	492	561	133	386	42
AO-900	483	445	103	319	23
AO-1100	458	130	28	96	6

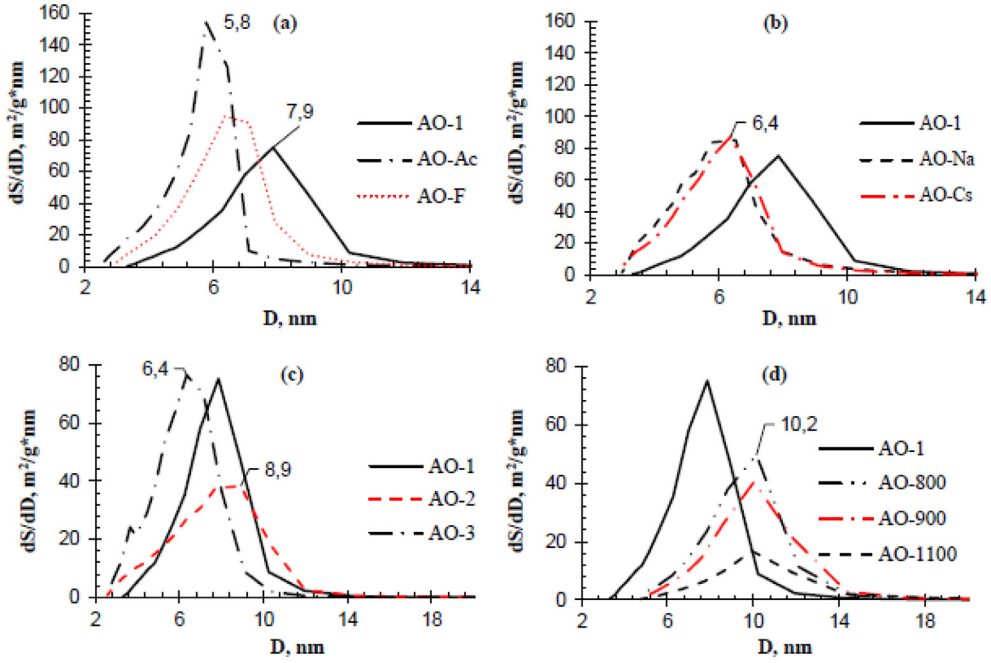

Fig. 6. The curves of surface area distribution over pore diameter of the aluminum oxides.

3.4. Methods for producing of phase-homogeneous γ-Al_2O_3 from the phase-inhomogeneous precursors

3.4.1. Hydrothermal treatment

Both aluminum hydroxide and aluminum oxide can be hydrothermally treated. Phase-homogeneous boehmite was obtained after hydrothermal treatment of the initial aluminum hydroxide within 4 h. Narrow high-intensity lines corresponding to boehmite are observed on the XRD pattern of the obtained AH-HTT sample (Fig. 1). The interlayer water content is 1.04 mol per 1 mol of alumina. The value of interplanar spacing (020) is 0.611 nm, which is typical for well-crystallized boehmite. There is no shoulder on the DSC curve, and there is a symmetric endothermic effect of the phase transformation of boehmite with a peak at 481 °C (Fig. 2d). As a result of such HTT, the crystallite size increases from 3.9 to 8.9 nm, which leads to a decrease in the specific surface area from 261 to 147 m^2/g (Table 1), a homogeneous system is formed with a maximum on the differential curves at 7.2 nm (Fig. 5c). For the AH-HTT sample, there are no characteristic bands on the IR spectrum at 1629 and 1379 cm^{-1} and the carbon content decreased to 0.05 wt %, which refers to physically adsorbed CO_2 from the air. Heat treatment of such sample at 550 °C leads to formation of phase-homogeneous γ-Al_2O_3 with a specific surface area of 169 m^2/g. It should be noted that the granules of aluminum hydroxide are quite fragile and can be destroyed under HTT conditions. Therefore, it is desirable to carry out hydrothermal treatment of the aluminum oxide.

In the case of HTT of the phase-inhomogeneous aluminum oxide, in 1 h amorphous alumina completely dissolves into fine crystalline boehmite and a certain fraction of γ-Al_2O_3 into larger crystalline boehmite. This is evidenced by the presence of two corresponding peaks at 482 and 514 °C of the endothermic effects of boehmite dehydration in γ-Al_2O_3. The content of the first boehmite is 38% and it corresponds to the amount of the amorphous phase in the initial AH-1 sample. That suggests that crystallization of amorphous alumina under HTT conditions is complete within 1 h. The content of larger crystalline boehmite is 11%, the rest is γ-Al_2O_3. The presence of boehmite and γ-Al_2O_3 is confirmed by XRD data [33]. The heat treatment of such sample at 550 °C leads to formation of phase-homogeneous γ-Al_2O_3, which specific surface area is 14% higher than unmodified alumina (Table 1, AO-3 sample).

3.4.2. High-temperature treatment of the phase-inhomogeneous aluminum hydroxide

Amorphous alumina is crystallized as a result of the initial aluminum hydroxide heat treatment at 800 °C, as evidenced by only one endothermic effect of the boehmite phase transformation on the DSC curve after HTT of AO-800 sample. The calcination of the initial aluminum hydroxide at 900 and 1100 °C is accompanied by formation of a mixture of crystalline aluminum oxides: ($\gamma + \delta$)-Al_2O_3 (ICDD PDF card 00-004-0877 for δ-Al_2O_3) and ($\theta + \alpha$)-Al_2O_3 (ICDD PDF card 01-079-1559 for θ-Al_2O_3 and ICDD PDF card 01-076-7775 for α-Al_2O_3) (Fig. 1c and d), respectively, with larger crystallite sizes (Table 1). Phase transformations within high-temperature treatment of the aluminum hydroxide are accompanied by compaction and growth of structure-forming fragments in oxides by the mechanism of coalescence sintering of pores [48]. This leads to a decrease in the values of the specific surface area and pore volume (Table 1) with a monomodal pore structure with a maximum on the differential curve in the region of 10 nm (Fig. 6d).

3.5. Investigation of acidic surface properties of the alumina oxides

According to the results of temperature programmed desorption of ammonia (NH_3 TPD) analysis, the total concentration of acid sites ($\sum$N) of unmodified phase-inhomogeneous alumina is 819 μmol/g (Table 3). Aluminas obtained after HTT of the AO-1 sample or treatment of AH-1 with acid additives are characterized by higher concentration of acid sites. So, samples AO-3 (Fig. 7a) and AO-Ac (Fig. 7b) have higher temperature of complete desorption of ammonia (T_d^{NH3}) on the TPD profile, due to increase in the concentration and strength of acid sites with an energy of ammonia desorption of more than 150 kJ/mol (Fig. 7b, Table 3).

The concentration of strong acid sites in AO-3 sample increases from 117 to 164 μmol/g. This is a consequence of the fact that in the course of HTT, first of all, the amorphous phase is recrystallized to fine-crystalline boehmite, which upon calcination forms fine-crystalline γ-Al_2O_3. Small crystals have a more defective structure due to increase in the fraction of edges and the appearance of cation vacancies formed upon dehydration of the interlayer space in fine-crystalline boehmite [49]. The AO-Ac sample is characterized by the highest acidity, $\sum$N = 1044 μmol/g (Table 3). For this sample, an increase in the concentration of strong acid sites by 91% is observed. The presence of an electronegative fluorine ion in the AO-F sample increases the concentration of predominantly strong acid sites by 31% (Table 3).

The reduction in the concentration and strength of the acid sites of aluminum oxides is facilitated by modification of the initial aluminum hydroxide with basic additives, its hydrothermal or high-temperature treatment. A decrease in values of T_d^{NH3} on the TPD profile of the corresponding samples AO-Na, AO-Cs, AO-2, AO-800, AO-900, and AO-1100 (Fig. 7d) indicates a weakening of the strength of acid sites. The total concentration of acid sites on the surface of AO-Na and AO-Cs decreases by 33 and 57%, relative to the AO sample, and amounts to 552 and 356 μmol/g, respectively. Among high-temperature aluminas, the lowest concentration of acid sites is observed in the sample obtained at 1100 °C, $\sum$N = 458 μmol/g. The decrease in the acidity in aluminum oxides as a result of the mentioned above modification methods occurs mainly due to decrease in the content of strong acid sites (Table 3).

To reveal the nature of the acidity of aluminum oxides, the IR spectra of adsorbed pyridine were obtained for AO-Ac, AO-HTT, AO-Ac and AO-Cs (Fig. 8, Table 4). For all samples, absorption band ($\nu_{CC(N)}$) of the formed pyridine complex with Lewis acid sites at 1450 cm^{-1} is observed.

Bronsted sites were not found as there is no band at 1540 cm^{-1} [50]. For samples AO-HTT and AO-Ac, an increase in the concentration of strong acid sites is observed. For the last sample, their content increases by ~3 times, from 37 to 109 μmol/g. The AO-Cs sample is characterized by the lowest acidity, with a significant decrease in the concentration of weak sites. According to the results of IR spectroscopy of adsorbed pyridine, the patterns of changes in the concentration of acid sites in the samples are similar to the results of NH_3 TPD.

4. Discussion

Thus, based on the obtained results, the industrial sample of the initial aluminum hydroxide produced by the alcoholate technology is phase-inhomogeneous and it consists of boehmite (62%) and an

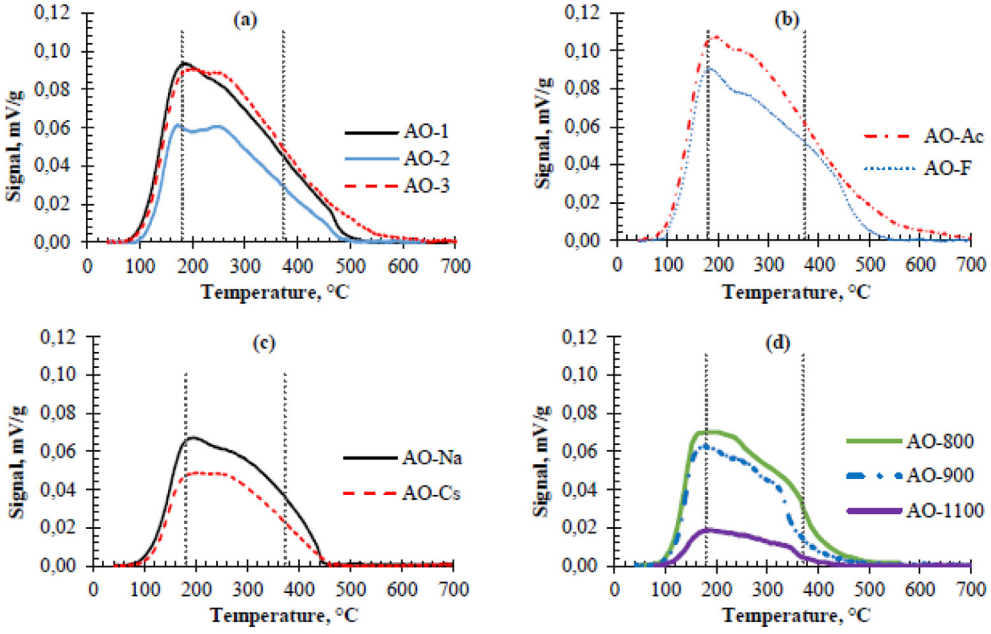

Fig. 7. NH_3 TPD profiles of the aluminum oxides.

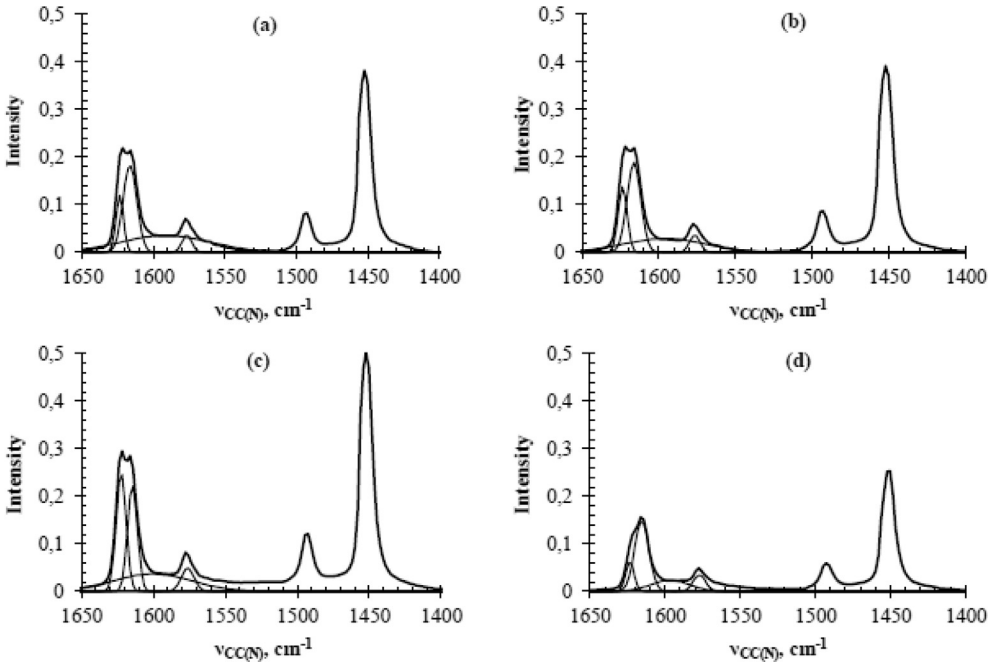

Fig. 8. IR spectra of adsorbed pyridine on the aluminum oxides: AO-1 (a), AO-3 (b), AO-Ac (c) and AO-Cs (d).

Table 4
Results from IR spectroscopy of adsorbed pyridine.

Sample	∑N, μmol/g	Weak ($\nu_{CC(N)} = 1596$ см$^{-1}$)	Medium ($\nu_{CC(N)} = 1616$ см$^{-1}$)	Strong ($\nu_{CC(N)} = 1623$ см$^{-1}$)
AO-1	265	125	103	37
AO-Ac	331	126	96	109
AO-Cs	170	44	100	26
AO-3	268	102	113	53

amorphous phase (38%) stabilized by aluminoxanes. Modification of aluminum hydroxide by acidic or basic additives does not lead to a change in the phase composition of hydroxides and aluminum oxides. On the part of the texture characteristics, no significant changes are also observed, with the exception for the sample modified with acetic acid. For the latter sample the formation of the basic salts of aluminum acetates occurs, as a result of interaction mainly with the amorphous phase. A porous structure with a monomodal pore distribution of a smaller pore diameter ($D_{max} = 3.8$ nm) is formed and the pore volume decreases by 22%. The heat treatment of such sample at 550 °C allows obtaining aluminum oxide, the specific surface area of which is 21% higher than of unmodified sample. The heat treatment at 550–650 °C of the initial and modified aluminum hydroxides is accompanied by formation of phase-inhomogeneous aluminum oxide, which consists of γ-Al_2O_3 and amorphous aluminum oxide. The effect of chemical modifiers is aimed at changing the acidity of the alumina. The use of acetic acid leads to formation of basic salts of aluminum acetate, the decomposition of which in the course of heat treatment leads to formation of defective structure alumina with a high concentration of all acid sites. The introduction of an electronegative fluorine ion promotes an increase in the concentration of strong acid sites due to the influence of fluorine on the near and far coordination spheres of aluminum cations [51,52]. The use of basic modifiers reduces the concentration and strength of acid sites. This is the result of electron density donation from modifying atoms to aluminum cations and the ability of modifying atoms to prevent the formation of cationic vacancies during calcination of modified aluminum hydroxides [36]. The greatest decrease in the acidity is facilitated by the introduction of cesium, as the strongest base.

The preparation of phase-homogeneous γ-Al_2O_3 was achieved by the methods of (i) HTT of aluminum hydroxide or alumina, followed by heat treatment at 550 °C and (ii) heat treatment of the initial aluminum hydroxide at 800 °C. The production of phase-homogeneous boehmite was achieved within 4 h of HTT of aluminum hydroxide, due to implementation of the dissolution-precipitation mechanism: amorphous aluminum hydroxide dissolves with the formation of aluminum hydroxocomplexes $Al(OH)_4^-$ and their deposition on crystals of existing boehmite.

$Al(OH)_3^{Am} + OH^- \leftrightarrows Al^{3+} + 4OH^- \rightarrow Al(OH)_4^- (pH = 7) \rightarrow$ γ-$AlOOH + 2OH^- + H^+$ [53,54].

Comparison of textural characteristics of the initial aluminum hydroxide and the phase-homogeneous boehmite showed that the amorphous phase is a source of a finely porous component with a pore diameter of ~3.8 nm, which contributes to an increase in the specific surface area of the sample by 78%, from 147 to 261 m^2/g. Analysis of the textural characteristics and acidity of unmodified alumina and phase-homogeneous AO-2 and AO-800 allows us to state that amorphous alumina causes an increase in the specific surface area by more than 12% and the concentration of acid sites by 32% mainly due to strong acid sites.

In the case of HTT of the phase-inhomogeneous alumina, crystallization occurs through the formation of a new phase – boehmite. During the HTT of AO within 1 h, fine-crystalline

boehmite is formed from aluminum hydroxocomplexes obtained as a result of predominantly dissolution of amorphous phase:

$Al_2O_3^{Am} + \gamma\text{-}Al_2O_3 + H_2O \rightarrow \gamma\text{-}AlOOH^{M} + n\ \gamma\text{-}AlOOH^{K} + (1\text{-}n)\ \gamma\text{-}Al_2O_3$.

Dehydration of fine-crystalline boehmite in γ-Al_2O_3 at 550 °C promotes an increase in the specific surface area in the AO-3 sample by 14% and the concentration of strong acid sites by 40%, when compared with unmodified AO sample. Earlier, we showed that the heat treatment of the products of the alumina HTT within the period longer than 1 h leads to formation of the phase-homogeneous γ-Al_2O_3 with low specific surface area and concentration of acid sites. The surface area of γ-Al_2O_3 obtained at 550 °C after HTT of AO-1 during 24 h is 116 m^2/g.

An increase of the calcination temperature of the initial aluminum hydroxide to 900 and 1100 °C leads to formation of alumina which consists of two crystalline phases and a significant decrease in the specific surface area, pore volume, and concentration of acid sites. The latter is due to a decrease in the fraction of cationic vacancies and the formation of well-crystallized phases.

Conclusions

This article shows that acidic and basic modifiers do not affect the phase composition of aluminum hydroxides and alumina which contain an amorphous phase. However, acetic acid is active in relation to the amorphous phase. This interaction leads to an increase in the specific surface area and concentration of acid sites in alumina. We found that the presence of about 40% of the amorphous phase promotes the growth of the specific surface area and the concentration of acid sites in alumina. The preparation of phase-homogeneous γ-Al_2O_3 is possible both as a result of HTT of aluminum hydroxide or alumina, and by the heat treatment of aluminum hydroxide at 800 °C. The advantage of the HTT method is the possibility of finer adjustment of textural and acid properties. In the case of a short-term HTT of a phase-inhomogeneous alumina and subsequent calcination, the values of these characteristics increase.

CRediT authorship contribution statement

A. Boretskaya: Writing - original draft, Writing - review & editing, Visualization, Investigation, Formal analysis. **I. Il'yasov:** Methodology, Validation. **S. Egorova:** Validation. **A. Popov:** Investigation. **A. Lamberov:** Resources, Supervision, Project administration, Funding acquisition.

Declaration of competing interest

The authors declare that they have no known competing financial interests or personal relationships that could have appeared to influence the work reported in this paper.

Acknowledgments

The work is performed according to the Russian Government Program of Competitive Growth of Kazan Federal University.

The thermal analysis of samples was carried out at the Federal Center for Collective Use of the Kazan Federal University with the support of A.V. Gerasimov, the Russian Agency for Science and Innovation.

References

[1] K.C. Popat, T.A. Desai, Alumina, in: B.D. Ratner, A.S. Hoffman, F.J. Schoen, J.E. Lemons (Eds.), Biomaterials Science: an Introduction to Materials in Medicine, third ed., Academic Press, 2013, pp. 162–166, https://doi.org/10.1016/B978-0-08-087780-8.00018-8.
[2] Shanker Ram, Metal Oxide Nanostructures as Gas Sensing Devices, G. Eranna, CRC Press, Boca Raton, FL, 2011, pp. 1277–1278.
[3] C.H. Bartholomew, R.J. Farrauto, N.J. Hoboken, Fundamentals of Industrial Catalytic Processes, Wiley, 2005.
[4] K.C. Taylor, Catal. Rev. Sci. Eng. 35 (1993) 457–481, https://doi.org/10.1080/01614949308013915.
[5] I. Levin, D. Brandon, J. Am. Ceram. Soc. 81 (8) (1998) 1995–2012, https://doi.org/10.1111/j.1151-2916.1998.tb02581.x.
[6] S. Liu, L. Zhang, L. An, J. Am. Ceram. Soc. 88 (9) (2005) 2559–2563, https://doi.org/10.1111/j.1551-2916.2005.00457.x.
[7] S.J. Tauster, S.C. Fung, R.L. Garten, J. Am. Chem. Soc. 100 (1) (1978) 170–175, https://doi.org/10.1021/ja00469a029.
[8] M. Delage, B. Didillon, Y. Huiban, J. Lynch, D. Uzio, in: A. Corma, F. V Melo, S. Mendioroz, J.L.G. Fierro (Eds.), 12th Int. Congr. Catal., Elsevier, 2000, pp. 1019–1024, https://doi.org/10.1016/S0167-2991(00)80332-8.
[9] P. Kirszensztejn, W. Przystajko, T.N. Bell, Catal. Lett. 18 (1993) 391–399, https://doi.org/10.1007/BF00765285.
[10] J. Lee, H. Jeon, D.G. Oh, J. Szanyi, J.H. Kwak, Appl. Catal. A Gen. 500 (5) (2015) 58–68, https://doi.org/10.1016/j.apcata.2015.03.040.
[11] M. Digne, P. Sautet, P. Raybaud, P. Euzen, H. Toulhoat, J. Catal. 226 (2004) 54–68, https://doi.org/10.1016/j.jcat.2004.04.020.
[12] Sposito Garrison, The Environmental Chemistry of Aluminum, CRC Press, 2020, 9780429606960.
[13] C.J. Brinker, G.W. Scherer, Sol–gel science, the physics and chemistry of sol–gel processing, Academic Press, Boston, 1990.
[14] A. Johansson, M. Roman, G.A. Seisenbaeva, L. Kloo, Z. Szabo, V.G. Kessler, J. Chem. Soc., Dalton Trans. 3 (2000) 387–394, https://doi.org/10.1039/A907720K.
[15] V.G. Kessler, in: Handb. Sol-Gel Sci. Technol., 2016, pp. 31–80, https://doi.org/10.1007/978-3-319-32101-1_1.
[16] B. Huang, C.H. Bartholomew, B.F. Woodfield, Microporous Mesoporous Mater. 183 (2014) 37–47, https://doi.org/10.1016/j.micromeso.2013.09.007.
[17] G.P. Belov, N.N. Korneev, Macromol. Symp. 97 (1) (1995) 63–78, https://doi.org/10.1002/masy.19950970107.
[18] C.C. Landry, N. Pappé, M.R. Mason, A.W. Apblett, A.N. Tyler, A.N. MacInnes, A.R. Barron, J. Mater. Chem. 5 (1995) 331–341, https://doi.org/10.1039/JM9950500331.
[19] M.R. Mani, R. Chellaswamy, Y.N. Marathe, V.K. Pillai, Chem. Commun. 51 (49) (2015) 10026–10029, https://doi.org/10.1039/c5cc01327e.
[20] M. Iaponeide, F. Macedo, C. Aparecido, B. Carla, C. Osawa, J. Mater. Sci. 42 (8) (2007) 2830–2836, https://doi.org/10.1007/s10853-006-1364-1.
[21] X. Zhang, Nanocrystalline Functional Alumina and Boehmite Materials: Synthesis, Characterizations and Applications, PhD Thesis, Tampere University of Technology, 2009.
[22] P. Katiyar, C. Jin, R.J. Narayan, Acta Mater. 53 (2005) 2617–2622, https://doi.org/10.1016/j.actamat.2005.02.027.
[23] G. Boisier, M. Raciulete, D. Samelor, N. Pebere, A.N. Gleizes, C. Vahlas, Electrochem. Solid State Lett. 11 (2008) 55–57, https://doi.org/10.1149/1.2968109.
[24] A. Ruys, in: Alumina Ceram., 2019, pp. 413–445, https://doi.org/10.1016/B978-0-08-102442-3.00013-0.
[25] M. Jiménez De Castro, R. Serna, J.A. Chaos, C.N. Afonso, E.R. Hodgson, Nucl. Instrum. Methods Phys. Res. Sect. B Beam Interact. Mater. Atoms 166–167 (2000) 793–797, https://doi.org/10.1016/S0168-583X(99)01178-7.
[26] J.L. Deschanvres, W. Meffre, J.C. Joubert, J.P. Senateur, F. Robaut, J.E. Broquin, R. Rimet, J. Alloys Compd. 742 (1998) 275–277, https://doi.org/10.1016/S0925-8388(98)00433-2.
[27] G.D. Stucky, P.D. Yang, D.Y. Zhao, D.I. Margolese, B.F. Chmelka, Nature 396 (1998) 152–155.
[28] V.B. Lazarev, G.P. Panasyuk, I.L. Voroshilov, G.P. Boudova, M.N. Danchevskaya, S.N. Torbin, Y.D. Ivakin, Ind. Eng. Chem. Res. 35 (10) (1996) 3721–3725, https://doi.org/10.1021/ie950404d.
[29] G. Amini, G.D. Najafpour, S.M. Rabiee, A.A. Ghoreyshi, Chem. Eng. Technol. 36 (2013) 1708–1712, https://doi.org/10.1002/ceat.201300102.
[30] A.H. Tavakoli, P.S. Maram, S.J. Widgeon, J. Rufner, K. Van Benthem, S. Ushakov, S. Sen, A. Navrotsky, J. Phys. Chem. C 117 (33) (2013) 17123–17130, https://doi.org/10.1021/jp405820g.
[31] K.V.P.M. Shafi, A. Ulman, J. Lai, N.L. Yang, M.H. Cui, J. Am. Chem. Soc. 125 (14) (2003) 4010–4011, https://doi.org/10.1021/ja0213625.
[32] A. Mavrič, M. Fanetti, G. Mali, M. Valant, J. Non-Cryst. Solids 466 (2018) 363–370, https://doi.org/10.1016/j.jnoncrysol.2018.07.055.
[33] S.K. Lee, S.B. Lee, S.Y. Park, Y.S. Yi, C.W. Ahn, Phys. Rev. Lett. 103 (2009), 095501, https://doi.org/10.1103/PhysRevLett.103.095501.
[34] H. Hashimoto, K. Yazawa, H. Asoh, S. Ono, J. Phys. Chem. C 121 (2017) 12300–12307, https://doi.org/10.1021/acs.jpcc.7b03629.
[35] A. Boretskaya, I. Il'yasov, A. Lamberov, A. Popov, Appl. Surf. Sci. 496 (2019) 143635–143643, https://doi.org/10.1016/j.apsusc.2019.143635.
[36] P. Berteau, M.A. Kellens, B. Delmon, J. Chem. Soc., Faraday Trans. 87 (9) (1991) 1425–1431, https://doi.org/10.1039/FT9918701425.

[37] R. Kosydar, A. Drelinkiewicz, E. Lalik, J. Gurgul, Appl. Catal. A Gen. 402 (1–2) (2011) 121–131, https://doi.org/10.1016/j.apcata.2011.05.036.
[38] Z. Wang, W. Wu, X. Bian, Y. Wu, Green Process. Synth. 5 (2016) 305–310, https://doi.org/10.1515/gps-2015-0128.
[39] S. Brunauer, P.H. Emmett, E. Teller, J. Am. Chem. Soc. 60 (2) (1938) 309–319, https://doi.org/10.1021/ja01269a023.
[40] S.J. Gregg, K.S.W. Sing, Adsorption, Surface Area and Porosity. 2. Auflage, Academic Press, London, 1982.
[41] V.V. Yushchenko, C.J. Vanegas, B.V. Romanovskii, React. Kinet. Catal. Lett. 40 (1989) 235–240, https://doi.org/10.1007/BF02073799.
[42] M. Tamura, K.I. Shimizu, A. Satsuma, Appl. Catal. A Gen. 433 (2012) 135–145, https://doi.org/10.1016/j.apcata.2012.05.008.
[43] P.S. Santos, A.C.V. Coelho, H.S. Santos, P.K. Kiyohara, Mater. Res. 12 (2010) 437–445, https://doi.org/10.1590/s1516-14392009000400012.
[44] P.A. Storozhenko, G.I. Shcherbakova, A.M. Tsirlin, A.S. Murkina, M.S. Varfolomeev, M.G. Kuznetsova, M.V. Polyakova, O.P. Trokhachenkova, Inorg. Mater. 43 (2007) 320–328, https://doi.org/10.1134/S002016850703020X.
[46] A. Ayral, J.C. Droguet, J. Mater. Res. 4 (4) (1989) 967–971, https://doi.org/10.1557/JMR.1989.0967.
[47] T. Sato, S. Ikoma, F. Ozawa, Thermochim. Acta 75 (1984) 129–137, https://doi.org/10.1016/0040-6031(84)85013-3.
[48] O.J. Whittemore, J.J. Sipe, Powder Technol. 9 (4) (1974) 159–164, https://doi.org/10.1016/0032-5910(74)80027-6.
[49] R.E. Smallman, A.H.W. Ngan, in: Mod. Phys. Metall., 2014, pp. 251–285, https://doi.org/10.1016/b978-0-08-098204-5.00006-7.
[50] M.I. Zaki, M.A. Hasan, F.A. Al-Sagheer, L. Pasupulety, Colloid. Surface. Physicochem. Eng. Aspect. 190 (3) (2001) 261–274, https://doi.org/10.1016/S0927-7757(01)00690-2.
[51] D.D. Eley, H. Pines, P.B. Weis, ss, 1966, ISBN 0080565204, 9780080565200.
[52] J. Xia, D. Mao, B. Zhang, Q. Chen, Y. Zhang, Y. Tang, Catal. Commun. 7 (6) (2006) 362–366, https://doi.org/10.1016/j.catcom.2005.12.011.
[53] F. Scholz, H. Kahlert, ChemTexts 1 (1) (2015) 1–7, https://doi.org/10.1007/s40828-015-0006-0.
[54] K. Wefers, C. Misra, Alcoa Tech. Pap. 19 (1987) 1–100.